

U.S.G.S. Earthquake Hazards Program Final Technical Report for External Research Support

U.S.G.S. Award Number: G15AP00011

Title of Award: THE ANALYSIS OF SCALING OF FAULT-RELATED PROCESSES: FLUID-ROCK INTERACTIONS and SLIP PROCESSES FROM THE MM TO 10'S KM SCALE OF SLIP WITHIN THE SOUTHERN SAN ANREAS FAULT SUBSIDIARY FAULT SYSTEM, MECCA HILLS, CA

Principal Investigators: James P. Evans (P.I.) and Kelly K. Bradbury (Co-PI), Department of Geology, Utah State University, Logan, UT 84322-4505

Award Term: January 1, 2015 – May 31, 2016

ABSTRACT

To examine how small faults may or may not scale to larger displacement faults, we examine a population of faults with a range of lengths and displacements that formed in the same tectonic regime, at nearly the same time. We characterize the fault structure, composition, and deformation mechanisms from across several map-scale faults within the Mecca Hills, southern California, and also examine small faults with a few centimeters of slip in the region. Comparison of our results to previous studies within the San Andreas fault system provides a range of analyses for faults with cm to several km of slip.

The northwest trending Mecca Hills east of the Salton Sea lie at the northern tip of a northwestern plunging anticlinorium cored by Proterozoic and Cretaceous gneisses and the Cretaceous Orocopia Schist. The Orocopia and its equivalent Rand and Pelona Schists (Jacobson, 1996) are exceptionally well-indurated formations that are locally metamorphosed to varying degrees and may include meta-sedimentary units with relatively low mica contents. The Orocopia foliation in the Mecca Hills study area has been modified by high-pressure metamorphism, and the faults that cut these rocks range in slip from cm's to several km's. Continuous transpressional deformation of the Mecca Hills and activation and cessation of these faults has resulted in exhumation shortly after they slipped, and provides excellent exposures of faults that formed in the same stress regime.

We use previous geologic mapping (Fattaurso et al., 2014; McNabb, 2013; Rymer, 1991; 1994; Boley et al., 1994; Sylvester and Smith 1976; Hays, 1957) and our new field work to shows where faults cut these crystalline rocks and conduct detailed sampling and structural measurements in an effort to characterize the nature and composition of the fault zones at the meter to sub-meter scale. Our studies consist of outcrop-scale structural analyses to determine the size and nature of deformation in the damage zone of the faults, examination of the microstructures, degree of fluid-rock interaction via measures of rock alteration, and stable isotope studies to evaluate the potential source of fluids that helped create syntectonic veins observed along the faults. We also collected several samples for testing several Fe- and Mn-coated slip surfaces for a new method of determining the maximum temperature of slip base on the changes in the redox state of Fe and Mn.

REPORT

Project results will be published across 3 individual papers to be submitted by the PI's, a USU M.S. student, and the 2 undergraduate students who have been partially funded on this research project. Portions of this work have been presented or are pending at several meetings including SCEC 2015 (Bradbury et al., 2015 and Moser et al., 2015); AGU 2015 (Bradbury et al., 2015 and Moser et al., 2015); SCEC 2016 (Bradbury et al., 2016 and Evans et al., 2016); and GSA 2016 (Evans et al., 2016 and Moser et al., 2016).

Significance of the Project

The field and laboratory based observations and measurements presented in this report provide information directly related to two of the research foci outlined in the 2015 NEHRP RFP (Priority Topic EP): 1) to address and quantitatively determine differences in the physical properties between plate boundary faults such as the San Andreas and smaller scale fault zones, and to further establish implications of fault zone 'maturity' for seismicity, and fault and earthquake mechanics; 2) to make field and laboratory measurements of fault zone structure, including damage, permeability, dilatancy, shear localization, alteration, mineralogy, roughness, shear zone width, and evolution of fault structure with accumulated offset and shear strain.

Characterization of the structural framework and fault-related rock properties of several faults within the Mecca Hills region of the Southern San Andreas Fault (SSAF) also provides a more detailed geologic context for recent geophysical studies that have shown: 1) the presence of a broad damage zone or reduced effective elastic moduli east of the main SSAF trace in the Mecca Hills area (Fialko, 2002; 2004; Cochran et al., 2009); 2) the importance of fault rock properties in the attenuation of near fault wave amplification (Roten et al., 2014) and the geometry of active fault structure (Fuis et al., 2012; Lin, 2013); and 3) the SSAF has a high probability of rupturing in a future large magnitude earthquake (Olsen et al., 2006) and locally exhibits creep (Lindsey et al., 2014; Roten et al., 2014).

Introduction

Numerous workers, examining a range of seismological data sets, support different interpretations as to whether small earthquakes exhibit self-similarity or exhibit a scale break at M 5-6 (Aki, 1967; McGarr 1999; McGarr et al., 2010; Ide and Beroza, 2001; Kwiatek et al., 2012; Boettecher et al 2009; Kanamori, 1993; Mayeda et al., 2005; Yamada et al., 2007; Yoo et al., 2013), or reflect processes that are highly variable depending on the nature of the stress state, fault structure, source processes, and detection capabilities (Shearer et al., 2006; Ide et al., 2003 vs. Prejean and Ellsworth, 2001). These interpretations give rise to key questions for understanding the processes by which earthquakes operate. The hypotheses, and the implications include: Are earthquake processes the same at all magnitude (length) scales? If the processes scale over magnitude and thus length scales, the processes interpreted from the laboratory and field sites can be extrapolated to understanding large earthquakes, if the appropriate scaling factor can be determined. This would allow insights from the controlled environments of lab tests, and the observations of many exhumed faults of modest displacements, to be used to help define the earthquake nucleation and rupture propagation process. If earthquake scaling breaks down, at what magnitude or length scale does the breakdown occur? If the breakdown occurs in the M 4-6 region, as suggested by Kanamori et al. (1993), this implies that analyses of source regions should focus on events with source areas of 3×10^3 to 3×10^7 m², or faults with lengths of ~ 100 m to 5.5 km, slip per event of 1 to 100 cm., and accumulated slip of a few cm to 100's m. What is the lowest magnitude where we still observe the self-similarity? If seismologists can resolve this question (See Mori et al., 2003; and Richardson and Jordan, 2002 vs. Boettecher et al., 2009; Kwiatek et al., 2011; for example) we can determine the smallest size event that can be produced in the lab, or is manifested in the field, that can then be applied to the larger rupture process, and the processes inferred from these studies might then inform analyses of earthquake forecasting. In this case, field-based analyses would extend to analyses at the microscopic and submicroscopic scales, if the concepts of picoseismicity hold (Ellsworth et al., 2007; Kwiatek et al., 2011) to M -3 and smaller.

Implicit in much of this work (and here we speak from our own bias) is that we assume that our studies of **small faults in the field or from other studies can** shed light on seismic processes, by making two key assumptions:

- 1) That the faults slipped at seismic slip rates in their evolution
- 2) The mechanisms processes that we infer from outcrop to microscale studies can be extrapolated to the scale of seismic slip nucleation and rupture, and can inform the geophysical community regarding the mechanisms, fluid flow, and stresses at great magnitudes.

If a Kanamori-like change in fault scaling occurs in the $\sim M = 6$ regime, we anticipate that larger faults would exhibit the result of more energy being focused within the central slipping portion of the faults, such as the presence of a thicker principal slip surface, evidence for frictional melt, and dimensions of key fault parameters that change nonlinearly with slip, such as damage zones that are narrower than what a linear [log-log] space would predict. Alternatively, if a McGarr-Ide model of self-similarity exists down to very small events, we should see evidence for rapid slip on even the smallest of faults, damage zones that scale with slip, and damage or fluid-rock interactions that scale with total slip.

These questions point to the need for field-based studies and sampling to determine how faults “age” – that is, how do fault structure, composition, and deformation microstructures vary from slip of < 1 cm to > 100 m. In using natural fault exposures as analogs for the seismic process, we should document that exhumed faults did indeed slip seismically. We aim to better constrain whether naturally exhumed faults are representative analogs for seismogenic faults and to add to and document/support the broader range of criteria that may be indicative of seismic slip in the rock record (Rowe and Griffith, 2015).

The Mecca Hills study area in southern California (Figure 1) is an ideal site to examine a set of multiple faults in proximity with a range of displacements (m’s to km’s scale slip) that formed at roughly the same depths, approximately the same stress state, and in association with the Southern San Andreas Fault (SSAF). The fault system exposed in the Mecca Hills region cuts crystalline bedrock (Figure 2) where several map-scale strike slip faults occur in an ~ 9 km wide zone east of the San Andreas fault. This fault system cuts the Orocochia Schist (Following Jacobson et al., 2007 the Pelona, Orocochia, and Rand Schists are interpreted to be equivalent sequences in the region) or Precambrian and Cretaceous crystalline rocks. In addition, small faults with cm to several m’s of offset cut the schists and gneiss and granitoids of the hills, and encompass faults with cm to > 1 km of slip. Long recognized for the deformation expressed in the sedimentary rocks of the area (Sylvester and Smith, 1976; Sylvester, 1999) the area also exposes steeply dipping right lateral, and right lateral oblique faults that cut the northern plunging nose of an Orocochia Schist cored anticline (Jacobson et al., 2007). The Mecca Hills do have the complexity of the fact that they are the type regions for the transpressional combination of right lateral and reverse slip (Sylvester and Smith, 1976; Sheridan et al., 1994) with some strike-slip deformation \pm contraction recorded in the crystalline rocks. However this contraction is also the cause of the uplift and erosion that creates the unique opportunity to see recently exhumed strike slip faults.

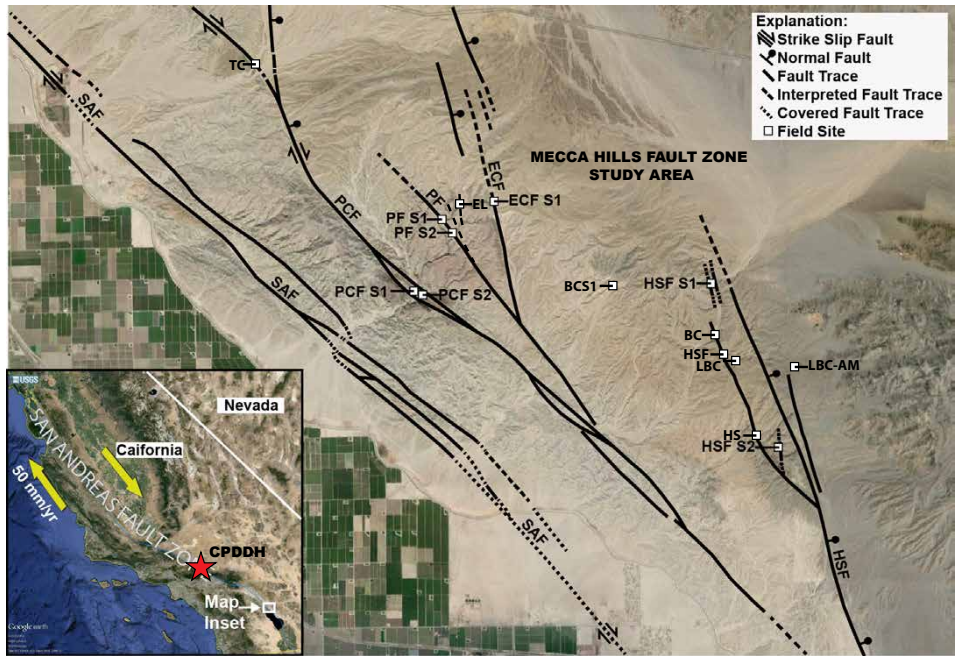


Figure 1. Location of Mecca Hills study area east of the Southern San Andreas fault (SSAF). Here numerous north to northwest trending strike slip and oblique slip faults occur within an ~ 9 km region east of the main San Andreas fault (SAF). Painted Canyon Fault (PCF), Platform Fault (PF), Hidden Springs Fault (HSF), Eagle Canyon Fault (ECF), and the Elvira Fault (ELF).

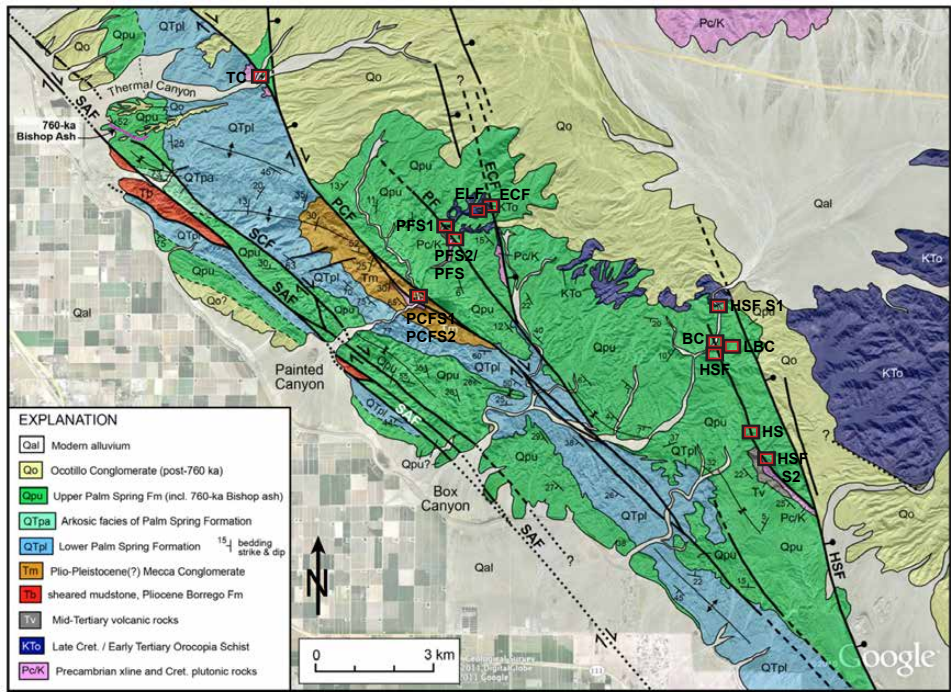


Figure 2. A recent geologic map of the Mecca Hills region by Fattaruso et al. (2014), based on new compilations (McNabb, 2013) and historical mapping (Sylvester and Smith, 1976, Rymer, 1991; 1994, Boley et al., 1994, and Hays, 1957). Boxes indicate our detailed study sites, sample localities, and/or transects across the faults.

METHODS

Mesosopic structural analyses

Analyses of outcrop scale structures provide clues into the evolution of structures, and indicate the localization of slip, as slip accumulates via the presence of early-formed structures that are later cut by localized faults. We characterize 4 map-scale faults across a ~ 9 km wide zone east of the Southern San Andreas in the Mecca Hills region (Figures 1- 2). Offset ranges from the meter's to several kilometer's scale, however, it is not well defined on some of these faults (see Sheridan et al., 1994; Rymer et al., 1994; Boley et al., 1994). Mesoscopic analysis is conducted in the NNE trending canyon exposures and road cuts that transect the faults, and in several cases, along the faults where deeply incised arroyos are parallel to the fault surfaces.

At the various field site localities, detailed fault transects consisting of measurements of shear zone widths and the orientation and distribution of vein systems, degree of alteration/mineralization, small fault distributions, and fracture characterization were conducted. A total of 300 samples, including host rocks, fault rocks and related damage zone elements (veins, slip surface coatings, fracture infillings), were collected for petrographic (thin-section, SEM chip and epoxy mounts), mineralogical (petrographic, SEM-EDS, XRD) and geochemical analyses (XRF and stable isotopes), and for potential future tests related to physical rock properties (V_p , V_s , elastic moduli, porosity, permeability).

Microstructural analyses

Transitions in fault processes as slip accumulates may become manifested in the deformation mechanisms that can be examined in the rock record. In addition, the analyses of synkinematic mineral assemblages (Jacobs et al., 2006) may provide broad constraints on the thermal structure of faults. These different methods provide some clues into the heat distribution associated with localized slip on faults, and the possibility of high temperatures due to fault rupture along very thin fault surfaces (Bustin, 1983; Sakaguchi et al., 2011).

We use optical petrography and scanning electron microscopy (SEM) imaging to characterize the textures and mineralogy, and to interpret the deformation mechanisms of and near the fault surfaces at the micron- to cm- scales. This work includes study of oriented samples, and deciphering between the alteration phases, microstructures, and the distribution of evidence for fluid flow along small veins and mineralized zones along the faults.

Mineralogical and Geochemical Analyses

Comparison of deformation-related alteration is measured on selected samples of veins and whole-rock material by systematic X-ray diffraction analyses (XRD) for mineralogy, and whole-rock chemistry performed by X-ray fluorescence analyses (XRF) to examine major, minor, and trace element chemistry. In the gneisses and schists of southern California, we focus on the presence of alteration-related phases, including clays, zeolites, micas, iron oxides, hydroxides, sulfides, and trace elements (e.g. Evans and Chester, 1995 or Schulz and Evans, 1998). Many of these phases indicate the alteration due to fluids (both fluid and vapor phases) in the fault zone, and can be used to propose retrograde reactions that produced such phases (Bradbury et al., 2011; Jacobs et al., 2006).

RESULTS

We examined 4 major fault strands (Painted Canyon fault; Platform fault; Eagle Canyon fault; Hidden Springs fault) and associated damage zones that are part of a classic palm-tree (Sylvester and Smith, 1976; Sylvester, 1988) or positive flower structure (Wilcox et al., 1993) formed from transpression along a strike-slip fault. This region of contractional uplift extends ~ 9 km to the east of the SSAF.

The results from the proposed Mecca Hills studies described below will be compared to our previous work on the San Andreas fault where it cuts crystalline bedrock (Tables 1 and 2). For example, in the San Gabriel Mountains, we examined the Punchbowl fault with as much as 44 km of offset, and documented the microstructures, geochemical alteration, and structure of the fault zone across three transects (Schulz and Evans, 1998; 2000). By investigating a series of exhumed fault zones with varying displacements yet within the same rock types and tectonic setting, results will provide an invaluable dataset on the structure and

physical properties of fault zones. The four faults we focus on here are:

Painted Canyon Fault

The Painted Canyon fault (PCF) may have 10-20 km of right lateral to right-lateral oblique slip (Sheridan et al., 1994) and is the largest and most significant fault in the Mecca Hills. It lies ~ 1.5 km east of the San Andreas fault, and cuts crystalline rocks and the Plio-Pleistocene sedimentary section (Figures 1-4). The Platform and Eagle Canyon faults splay off the PCF, and may have 1-4 km of right-lateral slip based on our preliminary mapping. The Hidden Spring and Grotto faults appear to tip out at their northern ends and have at most several 100 m of separation (Figure 2). A broad ~ 1.5 km wide damage zone is associated with the Painted Canyon Fault. Within the immediate damage zone surrounding the fault, numerous variegated and highly altered scaly clay gouge zones, hematite-coated slips surfaces, hydraulic brecciation and/or veining are pervasive (Figure 4-6).



Figure 3. Painted Canyon fault transect site. View is to the Southeast. The Painted Canyon fault is intensely deformed and consists of multiple strands of well-developed clay gouge zones (Figure 4). The fault zone geometry was mapped previously by Sylvester and Smith (1976) and Sylvester (1988).



Figure 4. Left: Multi-layered clay-rich fault gouge from location marked by red arrow in Figure 3. Right: Thin section microstructural analyses reveal brecciated veins with textures suggestive of hydraulic fracture. Hematite and magnetite mineralization may have formed synkinematically with deformation.

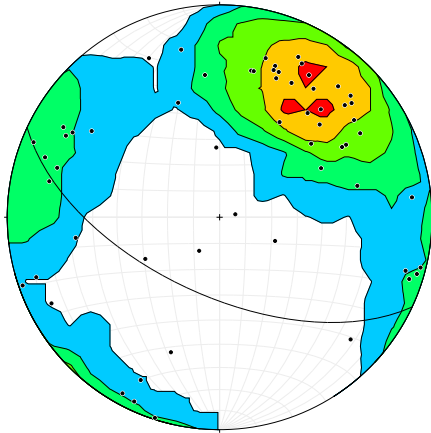
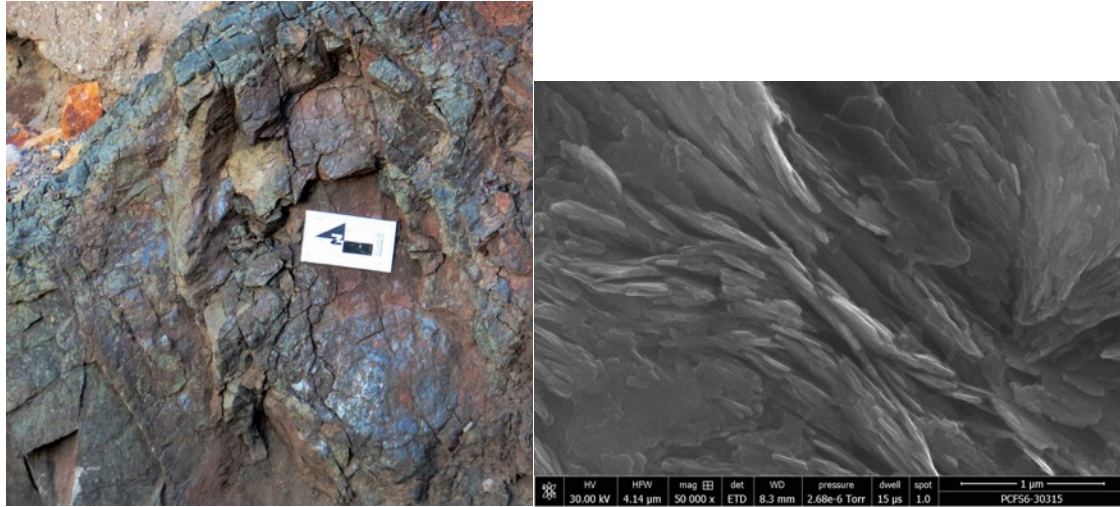


Figure 5. Upper Left Image: Small hematite-coated fault surfaces are common in the Painted Canyon Fault damage zone. The orientations of these structures roughly mirror that of the large Painted Canyon structure. Lower Right Image: Scanning electron microscopy images reveal nano-scale anastomosing slip surfaces with scaly morphology, suggesting that hematite mineralization occurred syn-kinematically. Kamb contour illustrates orientation of hematite-coated slip surfaces at the Painted Canyon Fault study site.

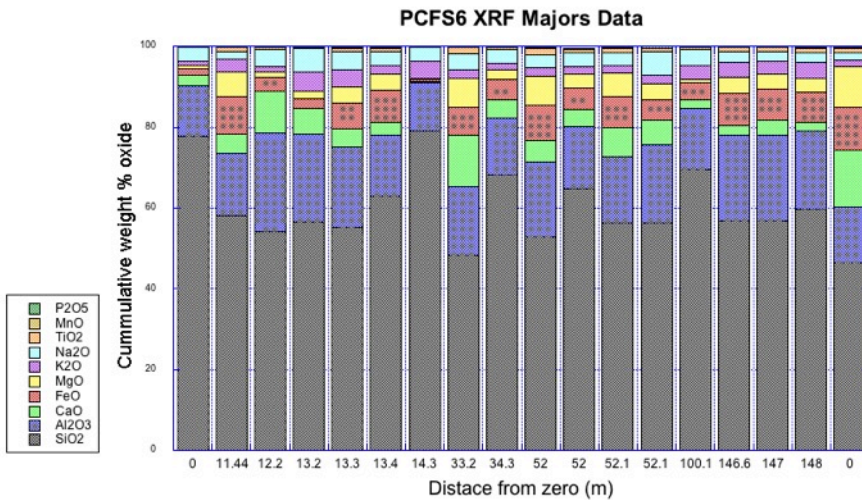


Figure 6. Geochemical analyses support the synkinematic mineralization hypothesis. Ca and Fe both generally increase from the protolith to fault related rocks. XRD analyses indicated Mg-rich clays (Palygorskite) and montmorillonite clays occur in the fault gouge with zeolite and hematite alteration minerals.

Platform Fault

Estimated right-lateral slip on the Platform fault is poorly constrained but at a minimum > 100 m with normal dip-slip displacement of ~ 150 m (Hays, 1957; Bryant, 2012). The Platform fault cuts Orocopia Schist and the overlying Plio-Pleistocene sedimentary section (Figures 1-2). Our analyses focuses on the sites near this sedimentary–crystalline rock contact. NE-SE trending fractures and small veinlets are present within the crystalline basement, however these veinlets do not extend into the sedimentary sequence. Small calcite veins do occur parallel to and just beneath the main slip surface which is SE-NW trending and steeply dipping (Figures 7-10). The immediate damage zone is more pervasive in the basement rocks to the west and extends for ~ 30 m, whereas to the east, the immediate damage zone is more pervasive in the sedimentary sequence and extends ~ 20 m. At all scales, deformation

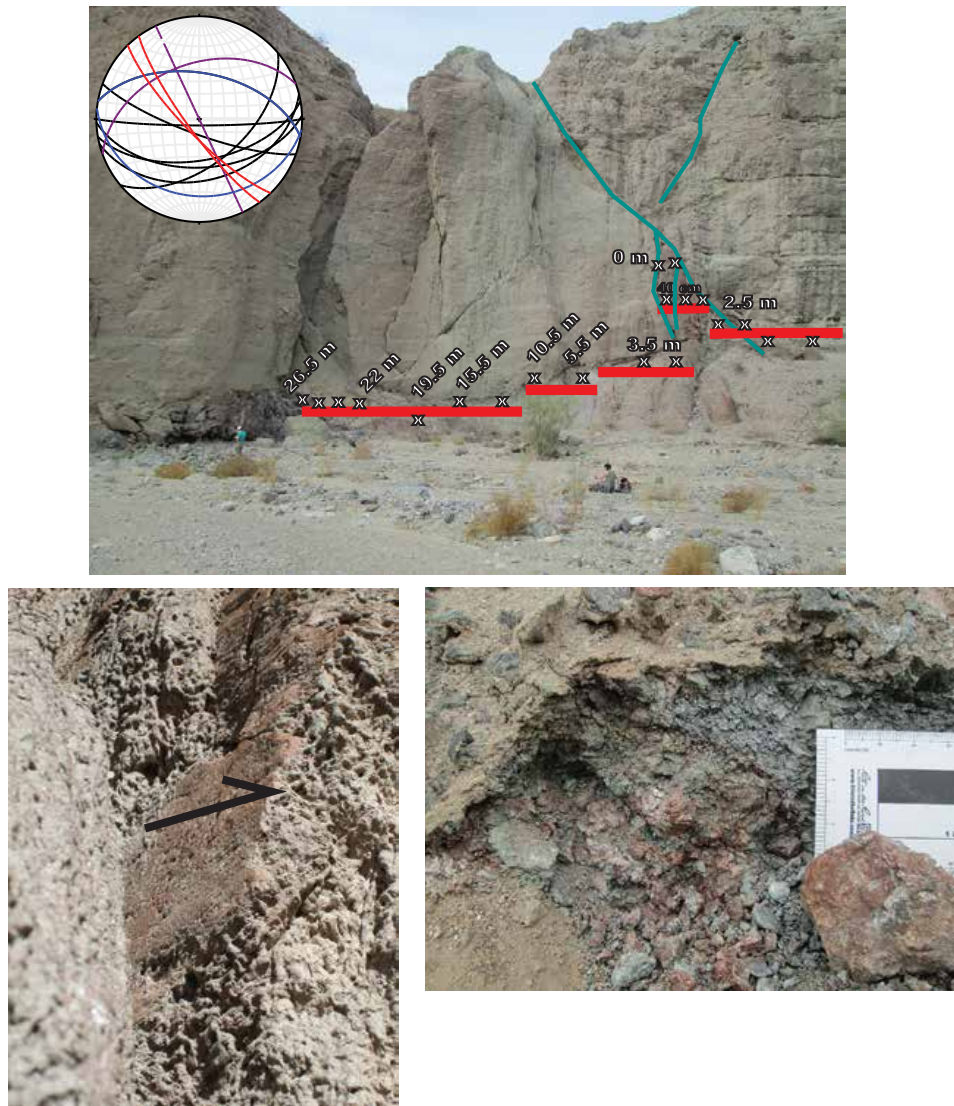


Figure 7. Measurements and sampling of the Platform fault across a 30-meter transect. Multiple 1-3 mm thick delicately clay coated slip surfaces are comprised of interlayered clays, chlorite-serpentine, clinochlore, and calcite with iron-oxide alteration. The slip surfaces are surrounded by a ~ 2 m wide zone of foliated scaly clay fault gouge (chlorite-serpentine-clinochlore-graphite-quartz) within the crystalline basement. The sedimentary sequence above the 0 m location was inaccessible to sampling. We have sampled the sedimentary sequence at several other localities (Figure 2).

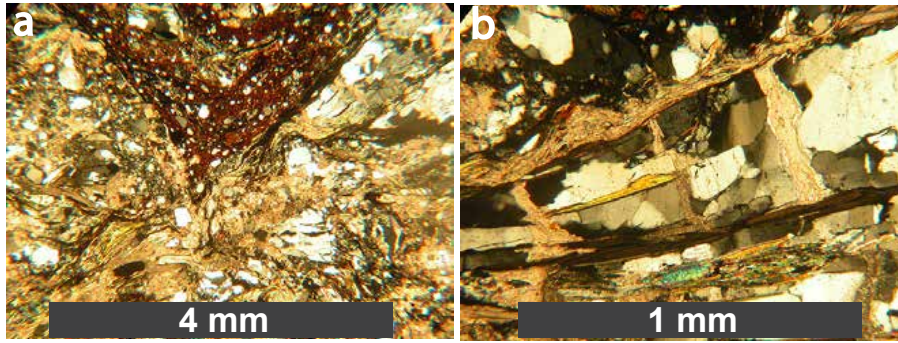


Figure 8. Left: Top of photo is the main Platform slip surface where fluidized cataclasite extends outward from slip surface. Right: Cataclasite layers offset by calcite veinlets both parallel and at high angles to slip direction and may represent deformation related to creep or triggered slip.

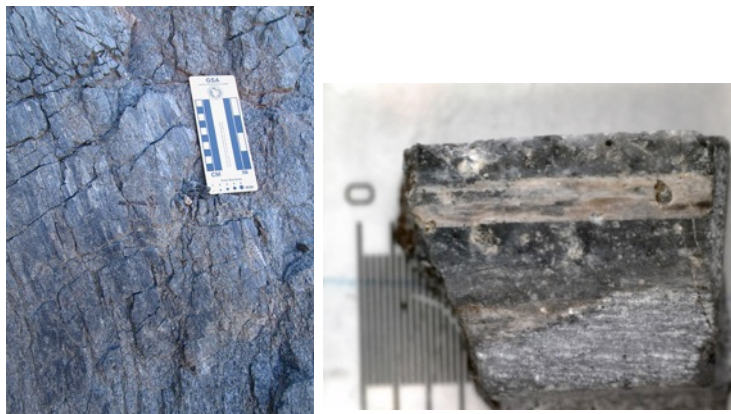


Figure 9. Highly reflective (mirror) SW-NE trending slip surfaces within Orocopia host rocks located between the Platform and Eagle Canyon faults (Figure 2). Reflective surfaces (left) may represent regions of elevated temperature as a result of seismic slip (Evans et al., 2014) and the etched/pitted textures (right) may indicate vapor phase activity.

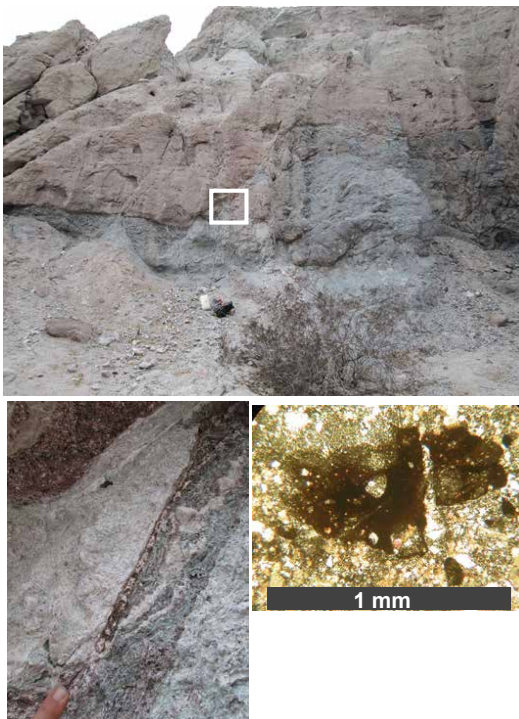


Figure 10. Outcrop photos of a smaller subsidiary normal fault ($230^{\circ}/57^{\circ}$ NW) within the immediate Platform fault damage zone with an estimated normal dip-slip displacement ~ 3 m. Central fault core gouge of this smaller scale fault is $\sim 5 - 10$ cm thick and consists of variegated red-brown-green-white clays and zeolites (laumontite). Photomicrograph of reworked ultra-cataclasite fragments within fine-grained cataclasite fault gouge. Calcite veinlets dissect multiple cataclasite fragments.

Hidden Springs Fault

The Hidden Springs Fault is > 20 km long, and our new work documents exposures of a well defined principal slip zone bounded by damaged Orocopia Schist. Our observations of the meso-scale structure of the north to northwest trending Hidden Springs fault zone (Figures 11-14) consists of multiple strands with well-developed clay-gouge zones bounded by 0.5 to 1 m thick gouge zones and 10's meters wide damage zones. Measurements across the fault in an east-west transect at the Box Canyon location include a central 20 cm thick scaly clay fault gouge bounded by a 1.5 m mixed clay gouge/cataclasite/ breccia zone which is in turn bounded by ~ 20 m wide mixed damaged zone within the sedimentary sequence. The contact between the Orocopia host and younger Quaternary - Tertiary sediments is marked by a 10 cm alteration iron-oxide/hydroxide rich halo. The deformation is asymmetrically distributed in the sedimentary rocks. On the main slip surfaces, white palygorskite slickenlines with multiple orientations of slip vectors are common (Figure 10). A north to northwest trending vein system parallels the fault within the Orocopia unit only and consists of quartz mineralization, hydraulic brecciation, and other phases, including calcite (Figure 12). A younger phase of east-west trending coarse blocky calcite veins is also present within ~ 5m of the fault contact into the Orocopia.

Another outcrop location of the Hidden Springs fault was also examined in Little Box Canyon (Figures 2 and 13-14). Here, the fault is observed in Q/T sedimentary sequence only. The relatively little amount of deformation that is expressed in the porous, poorly consolidated sedimentary sequences compared to the localities where basement rocks are cut by the same fault is notable.



Figure 11. Hidden Springs fault zone (HSF outcrop, Figure 2), Box Canyon Road. Left: USU Graduate student Amy Moser is sitting on the fault contact between the Cretaceous/Tertiary Orocopia Schist to the right and the younger Q/T sedimentary sequences to the left. Fine clays formed on the slip surface shown in the right photograph are palygorskite.

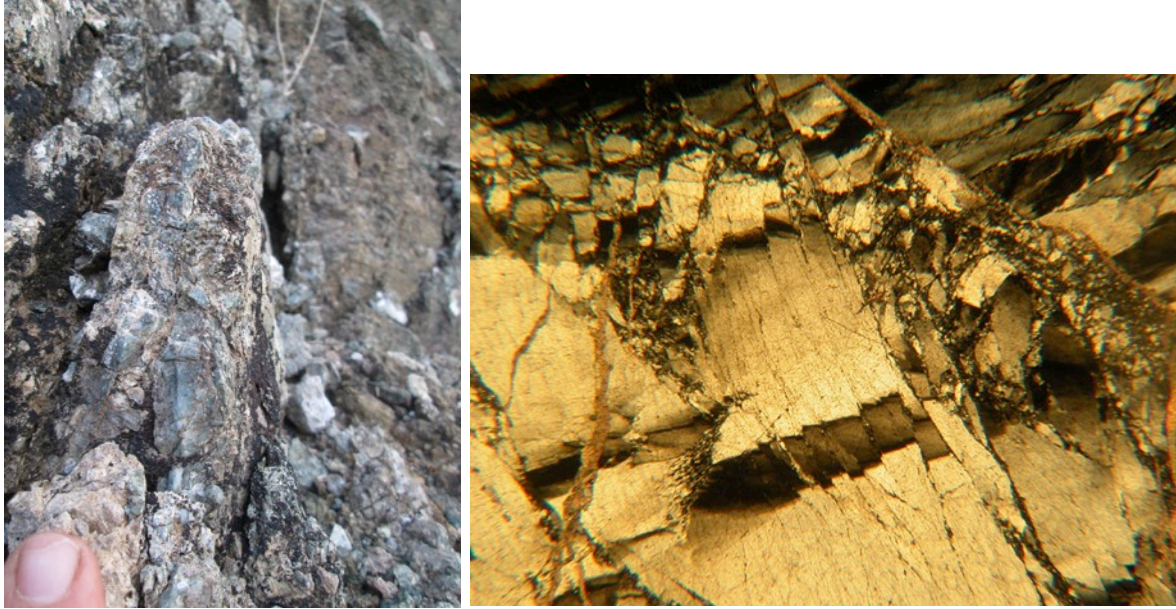


Figure 12. Quartz breccia vein within the damage zone of the Hidden Springs fault exposure in Box Canyon. Thin-section image highlights multi-episodic brittle deformation and development of cataclasite in the vein. Vein is crosscut by thin veinlets of calcite.



Figure 13. Left: Hidden Springs fault (Figure 2) exposure in Q/T sedimentary sequence south of Box Canyon. Right: At the outcrop scale, small slip surfaces with multiple orientations and curvilinear geometries exist throughout this exposure.

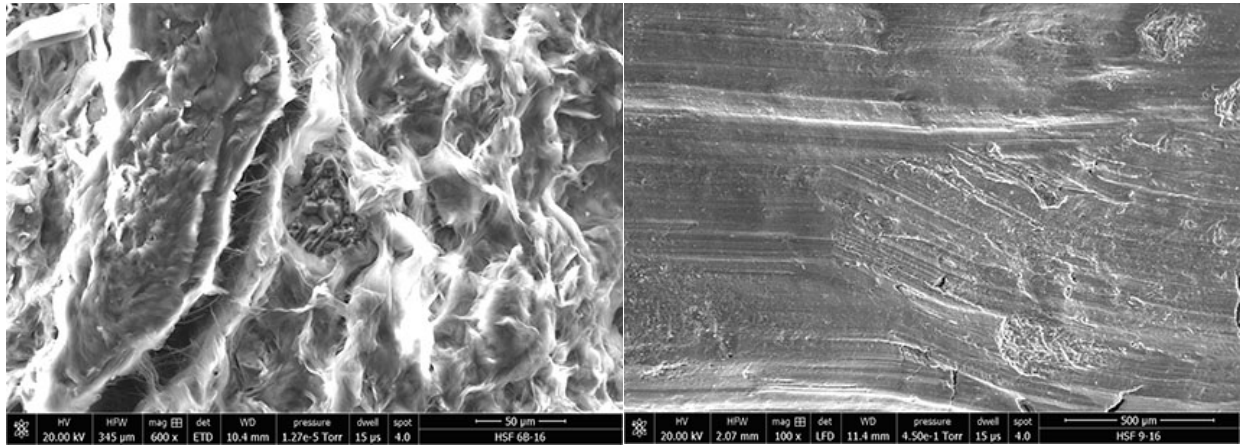


Figure 14. SEM images of slip surfaces at the Hidden Springs fault outcrop shown in Figure 12. Left: interwoven fabric of platy smectite (platy), palygorskite (fibrous, thread-like) on the slip surface at 600 x magnification; Right: texture of slip surface from Little Box Canyon Outcrop at 100x magnification shows multiple slickenline directions with a curvilinear trace, similar to the outcrop scale. Mineralogic composition based on XRD analysis of the slip surface indicates clinocllore, palygorsite, quartz, and calcite are all present.

Eagle Canyon Fault

The Eagle Canyon fault (Figures 15-17) is an oblique strike slip fault and may reach up to 100 m of vertical displacement (Hays, 1957). Well-developed clay and palygorskite rich slip surfaces are documented as are numerous veins and zones of alteration that suggest significant hydrothermal alteration and hydraulic brecciation related to deformation.

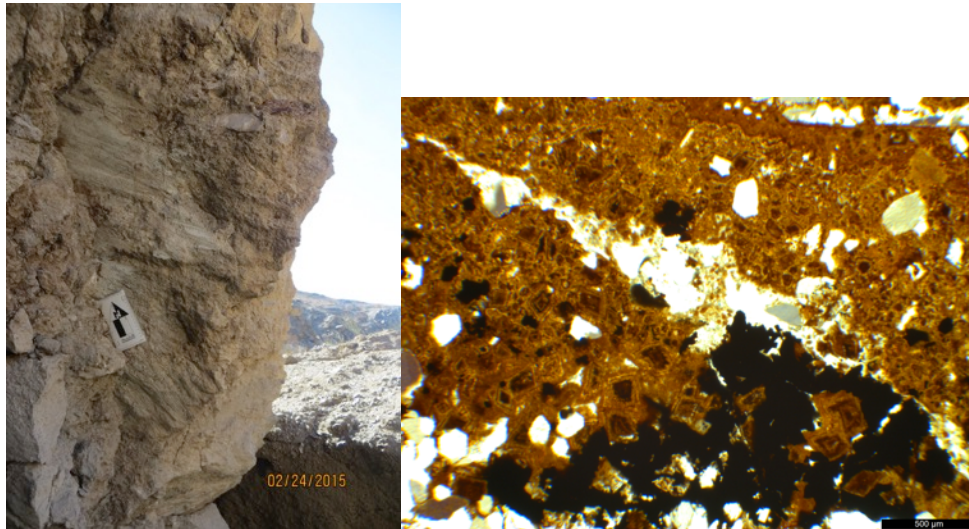


Figure 15. Left: Eagle Canyon Fault: main exposure of the Eagle Canyon Fault is a low angle shear zone enriched in ferroan dolomite (Right: thin section photo at 10x). The addition of ferroan dolomite in the fault zone also manifests in XRF geochemical analyses (Figure 17 - increases in Ca and Fe in the fault). Brecciated mixed zones and palygorskite slip surfaces (seds) are present at all fault exposures.



Figure 16. Left: Outcrop image of northwest trending steeply dipping vein system consist of multiple layers of fine clayey, matrix supported quartz hydraulic breccia and quartz. Right: thin section image of sample where field of view is 2.5 cm. XRD analyses shows the veins are comprised of quartz + calcite; dolomite + nontronite (Fe-rich clay) + clinocllore ± Cu-arsenates are identified in the brownish clayey matrix within the fractures and hydraulic breccia. Compositions of vein systems throughout the Mecca Hills are similar to hydrothermal mineral deposits identified further south near the Chocolate Mountains (e.g. Mesquite Mine).

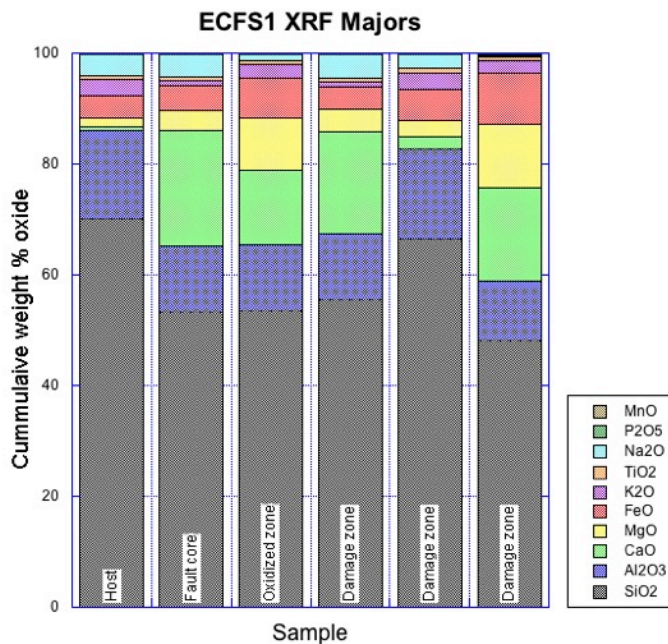


Figure 17. Whole-rock geochemistry of from XRF across the Eagle Canyon fault transect. A relative decrease in silica within the fault zone and surrounding alteration halos is observed.

Elvira Fault

The Elvira fault is one of many subsidiary faults observed between the Painted Canyon and Eagle Canyon fault zones. The orientation of the main slip surface varies from 026°/35°S to 050°/60° SE. Vertical and lateral displacements are poorly constrained. The main slip surface ~ 2.5 cm wide with a 2.5 m thick scaly clay gouge zone and a bounding 25 cm thick quartz breccia vein. The Orocopia crystalline basement is composed of quartz, clinocllore-Fe, muscovite, albite, ± calcite. Cataclasite gouge is composed of quartz, feldspars, clinocllore, calcite ± ankerite. Mineralogical and geochemical analyses of the quartz breccia vein also indicates the presence of calcite, graphite, and trace amounts of Cu and arsenates.



Figure 18. An example of a subsidiary fault between the Platform and Eagle Canyon fault. Here the Elvira Multiple 5 - 30 cm thick multi-layered cataclasite occurs along the sedimentary/Orocopia Schist fault interface.

Comparison to other Sites

Location of the proposed study area in the context of distribution of the Orocopia, Pelona, and Rand schists of southern California, and its relationship to the comparison sites along the Punchbowl Fault (yellow, Schulz and Evans, 1998; 2000; Chester and Logan, 1987) and Cajon Pass drill hole study of Forand (2010). Location of key sites for the San Gabriel and Punchbowl faults are shown for reference. Figure adapted from Jacobson et al. (2007).

We have examined in some detail the structure and composition of the Punchbowl fault where it cuts the Pelona Schist (Schulz and Evans, 1998; 2000). Here the fault has as much as 44 km of right-lateral slip, and was active 1-4 mya. Subsequent uplift has created exposures of the fault that represent conditions from 2-5 km deep. Transects from the Blue Cut exposure in the Cajon Creek area, and across the fault as exposed in fire roads in the mountains show that the damage zone of the fault is 100-200 m thick, with slip localization and shear reorientation, as determined from reorientation of primary schistose fabrics, in the 10-50 m region near the fault cores. In one site, multiple fault cores are present, each exhibiting its own damage zone.

Similar to the Punchbowl fault – faults in the Mecca Hills, at all scales, exhibit deformation mechanisms and textures that indicate slip localization by a combination of brittle faulting and preferred alignment along phyllosilicate-rich zones. Fluid-rock interactions are significant, and suggest hydrothermal alteration coupled with hydraulic brecciation as well as evidence for vapor phase processes.

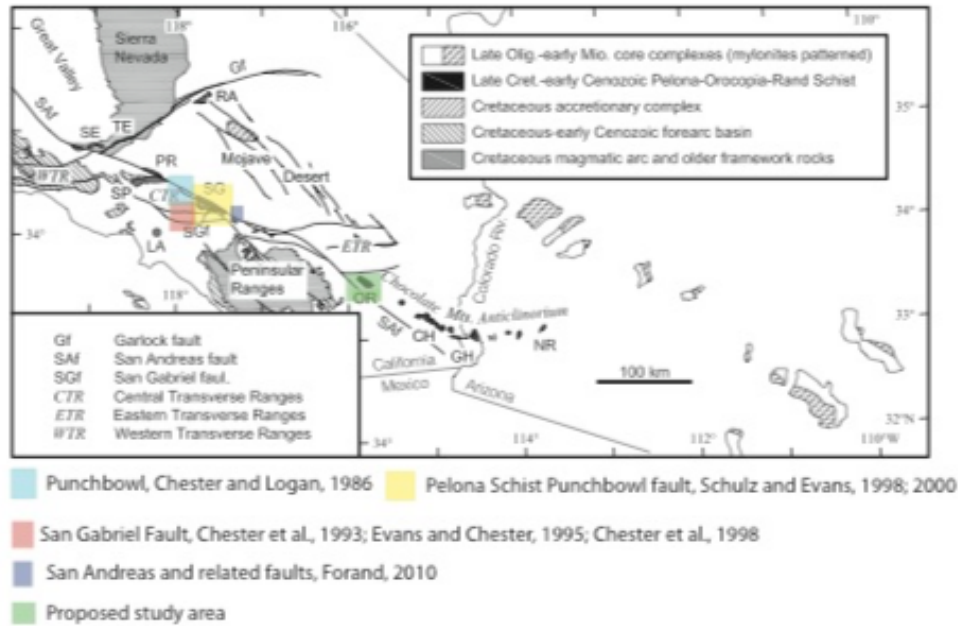


Figure 19. Location of fault zones discussed in this study (Table 1) and others (Table 2).

Table 1. Mecca Hills fault zone system examined in this project.

Fault Zone	Location and Structural Setting	Protolith	Structure	Texture/ Alteration/ Mineralogy
Painted Canyon	Mecca Hills, CA	crystalline basement, Q/Tseds	10-20 km's (?) right-lateral oblique slip; 1.5 km wide damage zone	Zeolites, nontronite clay, hematite
Platform	Mecca Hills, CA	crystalline basement, Q/Tseds	NW-SE / 80° dip; > 100 m right-lateral slip; multiple mm-thick surfaces surround by ~ 2 m thick foliated clayey fault gouge,	laumontite, calcite, clinochlore, chlorite-serpentine, epidote, magnetite, sulfides
Hidden Springs	Mecca Hills, CA	crystalline basement, Q/Tseds	NW-SE/78-90°; 1.2 km right-lateral displacement; multiple mm-thick slip surfaces within 1.5 m fault core thickness; 50-100 m damage zone thickness	Palygorskite, calcite, corrensite, clinochlore (Fe), quartz
Eagle Canyon	Mecca Hills, CA	crystalline basement, Q/Tseds	NNE trending, steeply east dipping; <100 m lateral displacement, > 100 m vertical displacement	Palygorskite, ferroan dolomite, quartz veins, calcite
Elvira	Mecca Hills, CA	crystalline basement, Q/Tseds	NE/35-60°; 2.5 cm fault core enveloped by 2.5 m thick clay gouge	Clinochlore (Fe), chlorite-serpentine, calcite,

Table 2. Comparison to other detailed sites examined throughout the region.

Fault Zone	Location and Structural Setting	Protolith	Structure	Texture/ Alteration/ Mineralogy	Reference/ Publication
Cleghorn	Cajon Pass, W. San Bernadino Mountains, CA	granite, granodiorite, gneiss	Drillcore	Laumontite	Forand, 2010
Cleghorn	W.San Bernadino Mountains, CA	granite	EW striking, steeply dipping, 3.5 km left-lateral offset; 32 cm fault core thickness; asymmetrical fault core; 9-60 m wide damage zone	Palygorskite, kaolinite, montmorillonite	Jacobs, 2006
Lakeview	Sierras, CA	crystalline basement, Miocene seds	NE-striking, moderately dipping; >180 m oblique slip; 90 - 130 cm fault core thickness; 2 main fault surfaces; oblique left and right lateral slip	Vermiculite- mixed layer smectite	
Grass Valley		granodiorite	39 m oblique slip; 2-12 cm fault core thickness;	Nontronite, Palygorskite	
Powell Canyon		gneiss	NW-SE striking, steeply dipping, 1.2 km right-lateral offset; related to SAF; >75 m damage zone	Feldspars, biotite, magnesio-hornblende	
Gemeni	East-Central Sierra Nevada, CA	granitoids	9.3 km trace length; 0-131 m slip ?	quartz-breccias; chlorite-epidote, quartz, sericitic, and muscovite	Pachell, 2002
Bear Camp	Central Sierras, CA	granodiorite	NE-striking, 33 m offset of dikes	chlorite-epidote, quartz	Robeson, K., 1998
Jim's Ridge	Central Sierras, CA	granodiorite	NE-striking, 19-30 m fault trace lengths, 41 to 5 cm offset, step-over geometry	chlorite-epidote, quartz	
	Sierra Nevada, CA	Granodiorite	10's to 100's m offset; relative strike slip displacement ~ 2 m; 0.1 - 10 mm fault core thicknesses	chlorite-epidote, biotite, sphene, calcite, zeolites	Lim, J., 1998
Punchbowl Fault	San Gabriels, CA		~ 44 km right-lateral slip; 100-200 m thick damage zone	Fe, Mn slip surfaces	Schulz and Evans, 1998; 2000 Chester et al., 2000

SUMMARY

We document that faults have slipped at seismic rates, and thus, we can use the field-based studies to examine seismic processes across a range of spatial scales. In the faults examined here, we observe a principal slip surface (PSS) that lies within a highly strained fault core zone (FC) along which most of the slip accumulates, surrounded by a zone of increased fracture and fault intensity known as the damage zone (DZ) (Chester and Logan, 1986; Caine et al., 1996). Although co-seismic slip may occur in the damage zone, or it may be the focus of aftershock activity, the PSS is the surface along which seismic ruptures must have propagated. Exhumed faults from seismogenic depths represent different stages of growth from small simple fault planes to large complex fault zones within a single lithology and due to one tectonic event (Evans et al., 2000).

Microstructures show an evolution from brittle fracture to cataclasis and formation of ultracataclasites with only a few meters of offset (Figure 10). Faults > 1 km long with over 100 m of net offset consist of several cm's thick scaly clay gouge zones and cohesive cataclasites. Mineralized fractures and shear zones in a ~ 0.5 to 2 m wide fault core are commonly bounded by thin (<mm) sub-parallel slip-surfaces. Vein systems throughout the damage zone trend parallel several of the main faults and contain hydraulic breccias and mineralization suggestive of hydrothermal fluids and/or vapor phase crystallization. Slip-weakening deformation and alteration mechanisms were active along the smallest faults with very low displacements, and the same mechanisms were responsible for slip in the largest faults.

The observations here show that there is little change in the composition and thickness and hence physical properties, of the PSS. This pattern of extremely localized slip is repeated in many other host rocks and tectonic settings. Large-displacement faults exhumed from near the top of the seismogenic zone (~5 km) associated with the San Andreas fault (Chester and Chester, 1998; Schulz and Evans, 1998; Bradbury et al., 2015), the Nojima fault (Ohtani et al., 2000), and the Median Tectonic Line (Wibberley and Shimamoto, 2003) show slip localized on a narrow zone less than 10 cm thick surrounded by a diffuse damage zone of smaller faults, fractures, and veins. Co-seismic ruptures with up to 10 m co-seismic slip on the Chelungpu fault are < 1 cm wide both in surface outcrops and in drill core from ~300m deep (Heermance et al., 2003). Natural earthquakes in South African mines produced microbrecciation zones 0.75 to 2.1 cm wide with 60 to 120 mm of slip (Gay and Ortlepp, 1979; McGarr et al., 1979; Ortlepp, 2000), and seismological studies there show events with $M = -2$ occur on thin fault patches (Kwiatek et al., 2011).

Experimentally formed faults also develop a narrow PSS. Narrow slip surfaces with well-developed foliated cataclasites and ultracataclasites develop at the margin of granite gouge samples with only mm of offset in the experiments of Yund et al. (1990) and Beeler et al. (1996). Experimental shearing of phyllosilicate-rich gouge also shows early slip localization (Bos et al., 2000; Scruggs and Tullis, 1998). Goldsby and Tullis (2002) show that sheared fine-grained fault material has low coefficients of friction. Thermal and chemical effects, microstructural evolution, and the development of wear particles may result in steady-state friction coefficients. The field and experimental observations suggest that these run-in phenomena are confined to the earliest phases of fault development and that once a PSS is established, lower friction coefficients often facilitate slip on existing mm to cm thick surfaces rather than the creation of new surfaces. In faults with km's of slip, damaged zones may be several 100 m wide, and consist of dense arrays of fractures, faults, veins, and altered rocks (Jacobs et al., 2006; Shipton et al., 2006). Damage zone deformation could be dynamic, caused either by stress changes during the passage of the rupture front or in events triggered by the radiated seismic waves in the near field.

A range of processes may consume energy within a fault zone, both on the active fault surface and in the damage zone around the main fault. Not all of these processes will occur along every fault in every earthquake. Additionally some of these processes may occur in the interseismic period, meaning that not all deformation mechanisms observed in exhumed faults are due to seismic slip events. Fault zone properties are highly variable in space, and may also vary in time between successive earthquakes. Whether or not any of these processes is active along a given fault will be dependent on a large number of factors such as host rock lithology, state of stress, dynamic and static friction values, depth, pressure, temperature and pore fluid pressure, mineralogy of the fault zone and geochemistry of the pore fluid.

To summarize our work in the Mecca Hills the main conclusions to date are:

- 1) Complex slip patterns occur with asymmetric damage zones, many fault surfaces dip < 90°

- 2) Significant hydrothermal fluid alteration associated with deformation is observed with the presence of numerous metalliferous elements detected
- 3) Range of structural features from micro- to meso-scale that suggest brittle deformation and creep processes occur
- 4) Geochemical signatures and textural features identified along several slip surfaces within the Mecca Hills suggest the potential for rapid, higher temperature slip events and vapor phase crystallization
- 5) We observe the development of damage zones, with considerable geochemical alteration, even for faults with relatively small amounts of slip. Faults at all scales exhibit principal slip surfaces, and geochemical and geochronologic evidence (*Moser, in prep.*) suggests that many of these faults likely experienced shear heating.

RELATED EFFORTS

This work is a part of our long-standing efforts to study faults in the context of the chemistry and physics of deformation. Starting with Chester et al. (1993), and continuing to today (Bradbury et al., 2011; 2015; Evans et al., 2014) we have examined faulted and deformed rocks from a wide range of settings in order to determine the degree and nature of fluid rock interactions (Evans and Chester, 1995; Goddard and Evans, 1995; Schulz and Evans, 1998), the structure of fault zones (Caine et al., 1996; Bradbury et al., 2011), the deformation mechanisms in the faults, the mechanisms of slip localization, the relationship between fault structure, chemistry (Hammond and Evans, 2003; Jacobs et al., 2006), and physical (Isaacs et al., 2008; Jeppson et al., 2010) and permeability properties (Caine et al., 1996; Evans et al., 1997; Shipton et al., 2002; Pasala et al., 2013; Petrie et al., 2014).

We have collected a substantial suite of fault-rock samples within the Mecca Hills region that extend from the crystalline basement rocks to the Quaternary/Tertiary sedimentary sequences. We hope to acquire funding to conduct future laboratory measurements of the mechanical properties and permeability of these rocks. We could then compare these results to previous and ongoing studies of fault rock properties within the SAF system (Bradbury et al., 2009; Jeppson et al., 2010).

An integrative structural, geochemical, and geochronological approach to investigate a suite of previously well-characterized faults in southern California provides a unique look into the thermal-chemical and stress evolution of exhumed brittle fault systems.

Transition Metal Paleothermometry

We collected fault surface samples for *Transition Metal Paleothermometry* along transects across the Painted Canyon, Platform, and Eagle Canyon faults and tested for transition metals using *X-ray Near-Edge Spectroscopy (XANES)* on two samples at the Stanford Synchrotron Radiation Laboratory (SSRL). We use these samples from this study area (though not funded by this project other than for the cost of field work and sampling) to determine the approximate temperatures of hydrothermal alteration and frictional heat produced along a few of these faults or small-scale slip surfaces. Evans et al. (2014) used X-Ray photoelectric spectroscopy (XPS) to estimate that 30% of the Fe³⁺ on hematite coated surfaces was reduced to Fe²⁺, and reflects a heating of at least 300°C, and perhaps much higher. The XPS method has several limitations for geologic analyses, in that it requires a very high vacuum that is difficult to obtain for many geologic samples.

The XANES analyses uses a synchrotron light source of X-rays that emits a highly focused, and extremely tuneable, beam of X-rays that examine the energy state of an area as small as 2 μm x 2 μm. This allows us to examine the distribution of different valence states of cations on a surface. The beam does not penetrate deeply, no sample preparation is needed, and no vacuum is required on the sample. This allows us to examine the distribution of and relative abundances of different valence states of metal cations. The work we have done to date consists of two days of beam time under a preliminary investigator status at SSRL. Mapping of an area ~ 1 cm² can take several hours, depending on the number of cations we examine and the resolution. Our hypothesis is that high temperatures produced either by shear heating across a mated surface, or at asperities, creates flash temperatures that create very localized reducing conditions, and reducing the valence state of the metal. For the faults in this study, we examined two samples, one from the Painted

Canyon Fault, and one from the Platform fault, for reduction of iron. Evans et al. (2014) suggest that small patches of iridescence correspond to places where this heating took place, and we sampled fault surfaces in the Mecca Hills for similar zones. Although not as well expressed as in other faults (Evans et al., 2015; Ault et al., 2015; McDermott et al., 2015; Channer et al., 2015) we did find numerous surfaces in the Mecca Hills that are candidates for further analyses.

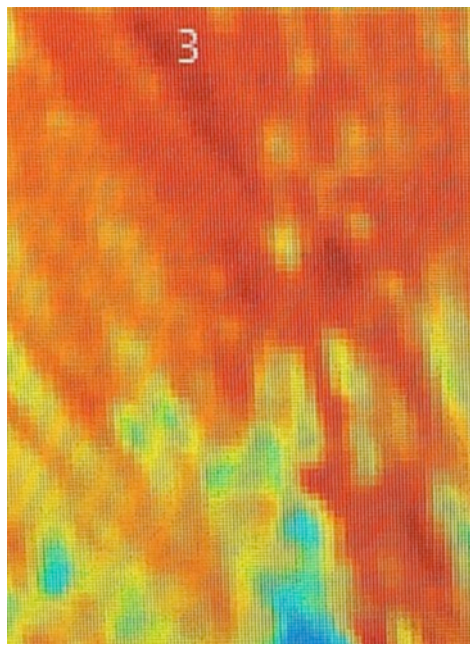


Figure 19. Preliminary results of XANES analysis from the SSRL shows that the Painted Canyon and Platform faults exhibit increased Fe^{2+} in places along the associated slip surfaces, with regions along these surfaces exhibiting significant changes in Fe oxidation. The hot colors indicate the presence of Fe^{2+} , where we posit that frictional heating has resulted in iron reduction. Field of view is 4 mm wide and 6 mm high.

STUDENT RESEARCH and METHODS TRAINING

Amy Moser, an M.S. candidate nearing completion at USU, has received significant support from this project and a large portion of her thesis is directly related to this project, in addition to the related efforts as discussed above. In addition, 2 USU undergraduate students (Sarah Schulties, B.S. 2016 and Kelsey Wetzel, B.S., 2017) were trained and/or assisted in various field and laboratory activities for this project. Laboratory training includes: 1) thin-section prep, including epoxy impregnation of poorly consolidated or fragile samples; 2) rock crushing and prep for XRD and XRF analyses; 3) SEM chip prep and epoxy ring mounts and sonicating/sterilization of samples; 4) attending short course and passing instrument and written tests to become authorized users on the Scanning Electron Microscope (SEM) at the Core Microscopy Laboratory within the USU Physics Department and 4) all sample preparation, weighing and acidification methods to conduct low-temperature stable isotope geochemistry.

ASSOCIATED PRESENTATIONS/MEETING ABSTRACTS

Bradbury, K.K., Evans, J.P., Moser, A.C., Schulthies, S.A., 2016, Multi-scale Structural Characterization of the Mecca Hills Fault System in the NE block of the Southern San Andreas Fault System, California, Poster Presentation at the 2016 Southern California Earthquake Center Annual Meeting.

Bradbury, K.K., Evans, J.P., Moser, A.C., Schulthies, S.A., 2015, Structural and Geochemical Characterization of Fault-related deformation in the Northeastern Block of the Southern San Andreas Fault, Mecca Hills, Southern California: American Geophysical Union Fall Meeting, Abstract T54B-01.

Bradbury, K.K., Evans, J.P., Moser, A.C., Schulthies, S.A., 2015, Structure and Mineralogical Characterization of Multiple Fault Traces in Painted Canyon Area, Mecca Hills, Southern San Andreas Fault System, California, Southern California Earthquake Center Annual Meeting, Abstract 258.

- Evans, J. P., Bradbury, K. K., Moser, A.C., Forand, D., and Ault, A., Chemical alteration of slip surfaces, linkages to coseismic weakening mechanisms, and dynamic weakening of faults.
- Evans, J. P., Bradbury, K. K., Moser, A., Janecke, S. and Forand, D. H., The development of inner damage zones around faults and their relationship to seismic attributes in faults: A virtuous feedback amongst seismicity, fluid flow, heat, alteration, and deformation, Geological Society of America national meeting, Denver, Sept. 25-28, 2016.
- Evans, J.P., Bradbury, K.K., Moser, A.C., Springer, S., Forand, D., and Jacobs, J., 2015, Analysis of San Andreas Fault Zone composition and structure: systematic mineralogic and structural studies: Geological Society of America Annual Meeting, Abstract 74-5.
- Evans, J. P., and Ault, A. K., 2015, Hot, Fast Faults: Evidence for High-Temperature Slip on Exhumed Faults, and Insights into Seismic Slip Processes, AGU Fall meeting abstract.
- Moser, A. C., Evans, J. P., Ault, A. K., Bradbury, K. K. and Janecke, S. U., Spatiotemporal evolution of San Andreas Fault-related deformation in the Mecca Hills, Southern California, from integrated fault zone characterization and low-temperature thermochronology, Geological Society of America national meeting, Denver, Sept. 25-28, 2016.
- Moser, A.C., Evans, J.P., Ault, A.K., Janecke, S.U., Bradbury, K.K., and Clausnitzer, S.M., 2015, Structural, Geochemical, and Thermal Evolution of the Southern San Andreas and Parallel Subsidiary Faults in the Mecca Hills, Southern California: Southern California Earthquake Center Annual Meeting, Abstract 274.
- Moser, A.C., Evans, J.P., Ault, A.K., Janecke, S.U., Bradbury, K.K., and Clausnitzer, S.M., 2015, Structural, Geochemical, and Thermal Evolution of the Southern San Andreas and Parallel Subsidiary Faults in the Mecca Hills, Southern California: American Geophysical Union Fall Meeting, Abstract T41A-2862.
- Moser, A. C., 2016, All I do are rocks, rocks, rock, Utah State University Ignite talk, April, 2016, ~ 250 attendees.
- Moser, A. C., 2016, TEDx talk, Geologic Insights into Life, TEDx symposium, Logan, Utah, October, 2016.

REFERENCES

- Aki, K., 1967, Scaling law of seismic spectrum, *Journal of Geophysical Research*, v. 72, p. 1217-1231.
- Andrews, D. J., Rupture dynamics with energy loss outside the slip zone, *J. Geophys. Res.*, 110, 14pp., 2005.
- Beeler, N. M., T. E. Tullis, M. L. Blanpied, and J. D. Weeks (1996), Frictional behavior of large displacement experimental faults, *J. Geophys. Res.*, 101, 8697-8715.
- Boettcher, Margaret S., McGarr, A., 2009, Johnston, Malcolm, Extension of Gutenberg-Richter distribution to MW -1.3, no lower limit in sight, *Geophys. Res. Lett.*, v. 36, <http://dx.doi.org/10.1029/2009GL038080>.
- Boley, J. L., Stimac, J. P., and Weldon, R. J., II, 1994, Stratigraphy and Paleomagnetism of the Mecca and Indio hills, Southern Ca., in: McGill, S. F., and Ross, T. M., eds, *Geologic Investigations of an active margin*, Geol. Soc. Am. Guidebook, p. 336-344.
- Bos et al., 2000
- Bradbury, K.K., Evans, J.P., Chester, J.S., Chester, F.M., and Kirschner, D.K., 2011, Lithology and internal structure of the San Andreas fault at depth based on characterization of Phase 3 whole-rock core in the San Andreas Fault Observatory at Depth (SAFOD) borehole: *Earth and Planetary Science Research Letters*, v. 310, no. 1-2, p. 131-144.
- Bradbury, K.K., Davis, C., Janecke, S.U., Shervais, J., & Evans, J.P., 2015, Composition, alteration, & texture of fault-related rocks from SAFOD core and surface outcrop analogs: evidence for deformation processes and fluid-rock interactions, *Pure Appl. Geophys.*, doi:10.1007/s00024-014-0896-6.
- Bryant, 2012, U.S.G.S.
- Bustin, R.M., 1983. Heating during thrust faulting in the Rocky Mountains: friction or fiction? *Tectonophysics* 95, 309-328.
- Caine, J.S., Evans, J. P., and Forster, C.B., 1996, Fault zone architecture and permeability structure: *Geology*, v. 24, no. 11, p. 1025-1028, doi:10.1130/0091-7613.
- Chester, F. M., and J. M. Logan, 1986, Implications for mechanical properties of brittle faults from observations of the Punchbowl fault zone, California, *Pure Appl. Geophys.*, 124, 79-106.
- Chester, F. M., and J. M. Logan, 1987, Composite planar fabric of gouge from the Punchbowl fault, California, *J. Struct. Geol.*, 9, 621-634.
- Chester, F.M., Evans, J.P., and Biegel, R.L., 1993, Internal structure and weakening mechanisms of the San Andreas fault: *Journal of Geophysical Research*, v. 98, p. 771-786.
- Cochran, E.S., Li, Y.-G., Shearer, P.M., Barbot, S., Fialko, Y., and Vidale, J.E., 2009. Seismic and geodetic evidence for extensive, long-lived fault damage zones, *Geology*, 37, 315-318
- Ellsworth, W., S. Hickman, M. Zoback, K. Imanishi, C. Thurber, and S. Roecker (2007). Micro- nano- and picoearthquakes at SAFOD: Implications for earthquake rupture and fault mechanics, *Eos Trans. AGU* 88, no. 52, Fall Meet. Suppl., Abstract S12B-05.
- Evans, J.P., and Chester, F.M., 1995, Fluid-rock interaction and weakening of faults of the San Andreas system: Inferences from San Gabriel fault-rock geochemistry and microstructures: *Journal of Geophysical Research*, v. 100, p. 13,007-13,020.

Evans, J.P., and D Forand, 2011, Discrete brittle to distributed shearing; Results from analysis of the deep portions of the Cajon Pass Drill Hole, Annual Meeting American Geophysical Union Abstracts.

Evans, J. P., Forster, C. B., and Goddard, J. V., 1997, Permeabilities of fault-related rocks and implications for fault-zone hydraulic structure, *J. Structural Geology*, v. 19, pp. 1393-1404.

Forand, D. H., 2010, Examination of Deformation in Crystalline Rock From Strike-Slip Faults in Two Locations, Southern California, M. S. Thesis, 181 p.

Fattaruso, L., Cooke, M., Dorsey, R., 2014, Sensitivity of uplift patterns to dip of the San Andreas fault in the Coachella Valley, California, *Geosphere*, v. 10, p. 1235-1246.

Fialko, Y., 2004, Evidence of fluid-filled upper crust from observations of postseismic deformation due to the 1992 M7.3 Landers earthquake, *JGR*, v. 109.

Fialko, Y., D. Sandwell, D. Agnew, M. Simons, P. Shearer, and B. Minster (2002), Deformation on nearby faults induced by the 1999 Hector Mine earthquake, *Science*, 297, 1858–1862, doi:10.1126/science.1074671.

Fuis, G.S., Scheirer, D.S., Langenheim, V.E., and Kohler, M.D., 2012, A new perspective on the geometry of the San Andreas fault in southern California and its relationship to lithospheric structure: *Bulletin of the Seismological Society of America*, v. 102, p. 236–251, doi:10.1785/0120110041.

Hays, W., 1957, *Geology of the Central Mecca Hills*, PhD Dissertation, Yale University.

Heermance, R. V., Z. K. Shipton, and J.P. Evans, Fault zone structure of the 1999 rupture on the Chelungpu fault, Taiwan, *Bull. Seis. Soc. Am.*, 93, 1034–1051, 2003.

Gay, N. and Ortlepp, W., 1979, The anatomy of a mining induced fault zone, *GSA Bulletin*.

Goldsby, D., and Tullis T., 2002, Low frictional strength of quartz rocks at subseismic slip rates, *GRL*, v. 29.

Ide, S., and G. C. Beroza, Does apparent stress vary with earthquake size?, *Geophys. Res. Lett.*, 28, 3349- 3352, 2001.

Ide, S., G. C. Beroza, S. G. Prejean, and W. L. Ellsworth, Earthquake scaling down to M1 observed at 2 km depth in the Long Valley Caldera, California, *J. Geophys. Res.*, v 108,

Isaacs A. J., J. P. Evans, P. T. Kolesar, T. Nohara (2008), Composition, microstructures, and petrophysics of the Mozumi fault, Japan: In situ analyses of fault zone properties and structure in sedimentary rocks from shallow crustal levels, *J. Geophys. Res.*, 113, B12408, doi:10.1029/2007JB005314

Jacobs, J. R., and Evans, J. P. and Kolesar, P. T., 2006, Chemical alteration in fault zones as sinks for “missing” earthquake energy, in: R. Abercrombie, H. Kanamori, and G. di Toro, eds., *AGU Monograph on Earthquake Energy*.p. 181-192.

Jacobson, C. E., Grove, M., Vucic, A., Pedrick, J. N., and Ebert, K. A. 2007, Exhumation of the Orocopia Schist and associated rocks of southeastern California: Relative roles of erosion, synsubduction tectonic denudation, and middle Cenozoic extension, *Geol. Soc. Am. Spec. paper* 419, 1-37.

Kanamori, H., E. Hauksson, L. K. Hutton, and L. M. Jones, Determination of earthquake energy release and ML using terrascopes, *Bull. Seism. Soc. Am.*, 83, 330-346, 1993.

Kwiatek, G., K. Plenkens, M. Nakatani, Y. Yabe, G. Dresen, and JAGUARSGroup (2011). Frequency- magnitude characteristics down to magnitude -4.4 for induced seismicity recorded at Mponeng gold mine, South Africa, *Bull. Seismol. Soc. Am.* 100, 1167–1173, doi [10.1785/0120090277](https://doi.org/10.1785/0120090277).

Kwiatek, G.; Plenkens, K.; Dresen, G. 2012, JAGUARS Res Grp, Source Parameters of Picoseismicity Recorded at Mponeng Deep Gold Mine, South Africa: Implications for Scaling Relations *BULL. Seis, Soc. Am.* v. 101p. 2592- 2608; [10.1785/0120110094](https://doi.org/10.1785/0120110094)

Lim, S. J., Small strike-slip faults in granitic rock: implications for three dimensional models, M.S. thesis, Utah State University, Logan, 136 p, 1998.

Lin, G., 2013, Three-dimensional seismic velocity structure and precise earthquake relocations in the Salton Trough, Southern California: *Bulletin of the Seismological Society of America*, v. 103, doi:10.1785/0120120286.

Lindsey, E. O., Y. Fialko, Y. Bock, D. T. Sandwell, and R. Bilham (2014), Localized and distributed creep along the southern San Andreas Fault, *J. Geophys. Res. Solid Earth*, 119, 7909–7922, doi:10.1002/2014JB011275.

Mayeda, K., R. Gok, W. R. Walter, and A. Hofstetter (2005). Evidence for non-constant energy/moment scaling from coda derived source spectra, *Geophys. Res. Lett.*, 32, L10306, doi:10.1029/2005GL022405.

McGarr, A., 1999. On relating apparent stress to the stress causing earthquake fault slip, *J. Geophys. Res.* 104,p. 3003– 3011, doi 10.1029/1998JB900083.

McGarr, A., and J. Fletcher, 2003. Maximum slip in earthquake fault zones, apparent stress, and stick-slip friction, *Bull. Seismol. Soc. Am.* 93,2355–2362, doi:10.1785/0120030037.

McGarr, A., J. Fletcher, M. Boettcher, N. Beeler, and J. Boatwright, 2010. Laboratory-based maximum slip rates in earthquake rupture zones and radiated energy, *Bull. Seismol. Soc. Am.*

McNabb, Stratigraphic record of Pliocene-Pleistocene basin evolution and deformation along the San Andreas fault, Mecca Hills, California, M.Sc. Thesis, U. Oregon, 69 p.

Mori, J., R. E. Abercrombie, and H. Kanamori (2003). Stress drops and radiated energies of aftershocks of the 1994 Northridge, California earthquake, *J. Geophys. Res.* 108, B11, 2545, doi:10.1029/2001JB000474.

Ohtani, T., K. Fujimoto, H. Ito, H. Tanaka, N. Tomida, and T. Higuchi, Fault rocks and past to recent fluid characteristics from the borehole survey of the Nojima fault ruptured in the 1995 Kobe earthquake, southwest Japan, *J. Geophys. Res.*, 105, 16161– 16171, 2000.

Olsen et al., 2006 Strong shaking in Los Angeles expected from southern San Andreas earthquake, *JGR-Solid Earth*, v. 33.

Pachell, M.A., Evans, J.P., 2002. Growth, linkage, and termination processes of a 10km-long strike-slip fault in jointed granite: the Gemini fault zone, Sierra Nevada, California. *J. Struct. Geol.* 24, 1903e1924.

Prejean, S. and W. L. Ellsworth (2001). Observations of earthquake source parameters at 2 km depth in the Long Valley caldera, eastern California, *Bull. Seism. Soc. Am.*, 91 165–177.

Richardson, E., and T. Jordan, 2002, Seismicity in deep gold mines of South Africa: Implications for tectonic earthquakes [10.1785/0120000226](https://doi.org/10.1785/0120000226), v. 92 no. 5 p. 1766-1782.

Rymer, M. J., 1991, The Bishop ash bed in the mecca Hills, in: Wallawender, M. J., and Hanan, B. J., eds., *Geol. Soc. Am. 1991 Field trip guide*, p. 388-396.

____ 1994, Quaternary fault-normal thrusting in the northwestern Mecca Hills, southern California, in : McGill, S. F., and Ross, T. M., eds, *Geologic Investigations of an active margin*, *Geol. Soc. Am. Guidebook*, p. 325-329.

Sakaguchi, , Chester, F., Curewitz, D., Fabbri, O., Goldsby, D., Kimura, G., Li, C.-F., Masaki, Y., Sreaton, E.J., Tsutsumi, A., Ujiie, K., Yamaguchi, A., 2011. Seismic slip propagation to the updip end of plate boundary subduction interface faults: vitrinite reflectance geothermometry on Integrated Ocean Drilling Program NanTroSEIZE cores. *Geology* 39, 395–398, <http://dx.doi.org/10.1130/G31642.1>.

Scruggs and Tullis, 1998

- Schulz, S. E., and Evans, J. P., 1998, Spatial variability in microscopic deformation and composition of the Punchbowl fault, Southern California: implications for mechanisms, fluid-rock interaction, and fault Morphology, *Tectonophysics*, v. 295,p. 223-244.
- Schulz, S. E., and Evans, J. P., 2000, Mesoscopic structure of the Punchbowl fault Southern California, and the geological and geophysical structure of active faults, *J. Structural Geol.* v. 22, p. 913-930.
- Sheridan, J. M., Weldon, R. J. II, Thornton, C. A., and Rymber, M. J., 1994, Stratigraphy and deformation history of the Mecca Hills, southern California, in: McGill, S. F., and Ross, T. M., eds, *Geologic Investigations of an active margin*, Geol. Soc. Am. Guidebook, p.319-325.
- Shipton, et al., 2014
- Sylvester, A.G., and Smith, R.R., 1976, Tectonic transpression and basement-controlled deformation in San Andreas fault zone, Salton Trough, California: *American Association of Petroleum Geologists Bulletin*, v. 60, p. 2081-2120.
- Sylvester, A. G., 1999, Rifting, transpression, and neotectonics in the central Mecca Hills, southern California, Pacific Section, SEPM Guidebook.
- Wibberley, C.A.J., Shimamoto, T., 2003. Internal structure and permeability of major strike-slip fault zones: the Median Tectonic Line in Mie Prefecture, Southwest Japan. *J. Struct. Geol.* 25, 59e78. Wibberley, C.A.J., Yielding, G., and Di Toro, G., 2008, Recent advances in the understanding of fault zone structure, In *The internal structure of fault zones: Implications for mechanical and fluid-flow properties*, Geological Society of London Special Publication 299, pp. 5-33.
- Wilcox et al., 1993
- Yamada, T., J. J. Mori, S. Ide, R. E. Abercrombie, H. Kawakata, M. Nakatani, Y. Iio, and H. Ogasawara, 2007, Stress drops and radiated seismic energies of microearthquakes in a South African gold mine, *J. Geophys. Res.*, 112, B03305, doi:10.1029/2006JB004553.
- Yoo, S., Harman, M. and Clark, D. 2013. Fault localization prioritization: Comparing information-theoretic and coverage-based approaches. *ACM Transactions on Software Engineering Methodology*. 22, 3 (Jul. 2013), 19:1–19:29.
- Yund et al., 1990